

## A New Compact, Light Weight Standing-Wave

### Linear Accelerator Structure

Eiji Tanabe, Matthew Bayer and Teresa Crockett  
Varian Associates Inc. Palo Alto, California, U.S.A.

#### ABSTRACT

A new compact, small diameter, light weight standing-wave linear accelerator structure suitable for industrial and medical application was developed. The new design utilized a shaped coaxial cavity as the coupling cavity. This structure offers a significant reduction in overall diameter over the side-coupled, annular ring, and existing coaxial coupled structures, while maintaining a high shunt impedance, large nearest-neighbor coupling and low next-nearest-neighbor coupling. A prototype accelerator designed to operate at S-band frequency was built and tested. A similar accelerator that is designed to operate at X-band frequency is currently under development. The theoretical accelerator design parameters, as well as experimental results, are presented.

#### INTRODUCTION

Existing standing-wave accelerator coupling cavities can be classified into four general design types: side cavity, on-axis, coaxial, and annular ring structures. These four structures are shown schematically in Figure 1 and important features are summarized in Table I.

Since the side cavity structures are off-axis, they do not influence the design of the accelerating cells, enabling side coupled accelerators to attain high efficiencies. Side coupled structures, however, have the disadvantages of increasing the effective diameter of the accelerator guide, lower  $K_1$  and a large number of machining and assembly steps required.

Cylindrically symmetric cavities - the on-axis, coaxial, and annular ring designs - have the advantage of being machined directly into the opposite side of an accelerating cell, thereby eliminating multi-piece assembly and prebrazing. Construction costs can be substantially reduced. Existing designs, however, all have disadvantages. The radius of an on-axis coupling cavity is comparable to the radius of the accelerating cavity, but the structure is susceptible to the excitation of parasitic and beam blowup modes, which reduce the overall accelerator efficiency and beam stability<sup>1</sup>. On-axis structures are also sensitive to thermal detuning, a result of the thermal deformation of the web between accelerating cells.<sup>2</sup> Coaxial structures eliminate the direct interaction of the electron beam with the coupling cavity, but existing designs increase the effective guide diameter 60% to 80%. The coaxial structure is also more resistant to thermal detuning. Current designs consist of narrow cylindrical cavities sandwiched between accelerating cells, which operate at a coaxial  $TM_{010}$ -like mode.<sup>3</sup> Coaxial cavities use magnetic coupling and have strong nearest-neighbor coupling,  $K_1$ , with small next-nearest-neighbor coupling,  $K_2$ , which

improves power flow and increases the mechanical tolerances allowed. Annular ring designs have the same size disadvantage as the existing coaxial structures, along with increased machining complexity. Moreover, these large diameter coupling cavities tend to excite higher order modes.

Coaxially coupled structures, however, attain a higher percentage of theoretical shunt impedance<sup>4</sup>. The size disadvantage of the annular ring and existing coaxial designs exemplifies the problem of developing a new coaxial design which 1) has a diameter comparable to an accelerating cavity, 2) does not significantly increase the web thickness, and 3) has large  $K_1$  and small  $K_2$ . In this paper, a new coaxial cavity design is presented, and low power tests of a prototypical accelerator using this design are summarized.

## THE COAXIAL COUPLED ACCELERATOR

### The Coaxial Coupling Cavity Design

The new structure is presented schematically in Figure 2. It consists of a small radius, coaxial structure with enlarged triangular areas which fill the unused areas between accelerating cavities and increase the magnetic induction in those regions. In essence, the geometry enhances the intrinsic field distribution of a simple coaxial cavity in the  $TM_{010}$ -like mode, while reducing the cavity to smaller overall dimensions. The flat area between the enlarged end regions acts as an effective capacitor and concentrates the electric field in that region, away from the coupling slots, similar to a reentrant cavity. The concentration of the magnetic field provides an ideal coupling opportunity. Two slots are cut  $180^\circ$  opposite each other, thereby preserving symmetry about the beam axis. Relatively small slots can provide adequate nearest-neighbor coupling,  $K_1$ , and the next-nearest-neighbor coupling,  $K_2$ , can be made negligibly small by rotating the slots  $90^\circ$  at each cell. The design also allows for a very high  $K_1$  to be obtained while keeping  $K_2$  to an acceptable value, by increasing the slot width and arc length.

### The Accelerator Design

An S-band prototype accelerator which consists of 7 1/2 accelerating cavities was designed for optimum performance at 4 MeV output energy. A beam simulation program was used to develop the buncher configuration for the guide, using the LALA field profiles. An injection voltage of 15 kV was used, with variable field gradients. The resulting output energy spectra are given in Figure 3. The overall length of the guide is 35.9 cm. The peak rf power delivered at the guide is 2.3 MW, with a 4.3 usec pulse width. Table II summarizes the accelerator design parameters. Both the coupling and accelerating cells were accurately tuned by machining, in order to make post-braze tuning of the guide unnecessary. The accelerating cells were tuned to within  $\pm 0.1$  MHz of the desired frequency. The desired frequencies were determined from the dispersion measurements of successive stacks of 2, 4, and 6 half cells. Because of the sensitivity of the large capacitive region of the cavity to gap length, the effect of the braze had to be allowed for. The full cavity frequency varies 240 MHz/mm of additional spacing between half cells. The braze process adds 20 microns of copper between cells on average, resulting in an increase of approximately 5 MHz.

An X-band accelerator currently under development, will consist of 12 1/2 accelerating cavities with an overall length of 19.7 cm. It is designed to have an output energy of 4 MeV and will be powered by a 1.3 MW coaxial

magnetron at 9300 MHz. Because of mechanical and thermal characteristics, and beam dynamics, the X-band accelerator design cannot be simply a scaled version of an S-band accelerator. The resultant shunt impedance is  $139 \text{ M}\Omega/\text{m}$  which is only 65% of the value for a simple scaled design.

#### EXPERIMENTAL RESULTS

The measured and theoretical dispersion curves for the brazed S-band accelerator guide are shown in Figure 4. The theoretical curve assumes a biperiodic structure with  $f_{\text{accelerating}} = 2996.69 \text{ MHz}$  and  $f_{\text{coupling}} = 3000 \text{ MHz}$ . The measured lowest higher order mode starts at 4300 MHz, far above the dominant mode. The guide had a measured  $Q$  of 13,500 and  $Q_{\text{ext}}$  of 6,580, with a coupling factor,  $\beta_0$ , of 2.05. The nearest-neighbor coupling,  $K_1$  was 3.3% and the next-nearest-neighbor coupling,  $K_2$ , was 0.04%. The coupling cavity frequencies were  $3001.5 \text{ MHz}, \pm 1.5 \text{ MHz}$ . Before and after brazing length measurements of the guide indicated a greater than average increase per cell, approximately 30 microns. This explains the high coupling cavity frequency, which is apparent in the dispersion curve. The accelerating cells remained tuned to within  $\pm 0.1 \text{ MHz}$  of a fixed frequency. These frequency variations were acceptable and no post-braze tuning of the guide was done. High power tests of the accelerator are currently being undertaken.

#### CONCLUSION

A new, small diameter coaxial coupling cavity which fits entirely in the web between accelerating cavities was developed. A compact, standing wave, linear accelerator incorporating the new cavity was designed, assembled, and tested. In addition to smaller size and less weight, the accelerator offers various advantages over existing structures. The component cells are simpler to machine and assemble. No post-braze tuning of the accelerator is required. For equal size coupling slots, higher values of  $K_1$  with lower values of  $K_2$  are obtained. Because of the small coupling cavity diameter, the frequencies of higher order modes lie well above the dominant mode frequency. Low power tests indicated the properties of the assembled prototype accelerator were in good agreement with the design calculations.

#### REFERENCES

1. J. P. Labrie and J. McKeown, "The Coaxial Coupled Linac Structure", Nuclear Instruments and Methods, No. 193, pp. 437-444, 1982.
2. J. McKeown and J. P. Labrie, "Heat Transfer, Thermal Stress Analysis and the Dynamic Behavior of High Power RF Structures", IEEE Transactions on Nuclear Science, Vol. NS-30, No. 4, pp. 3593-3595, 1983.
3. R. M. Laszewski and R. A. Hoffswell, "Coaxial-Coupled Linac Structure for Low Gradient Applications", in Proceedings of the Linear Accelerator Conference 1984, pp. 177-179.
4. S. O. Schriber, et al, "Effective Shunt Impedance Comparison Between S-Band Standing Wave Accelerators with On-Axis and Off-Axis Couplers", in Proceedings of 1976 Proton Linac Conference, Atomic Energy of Canada, Ltd. Report No. AECL-5677, 1976, pp. 338-343.

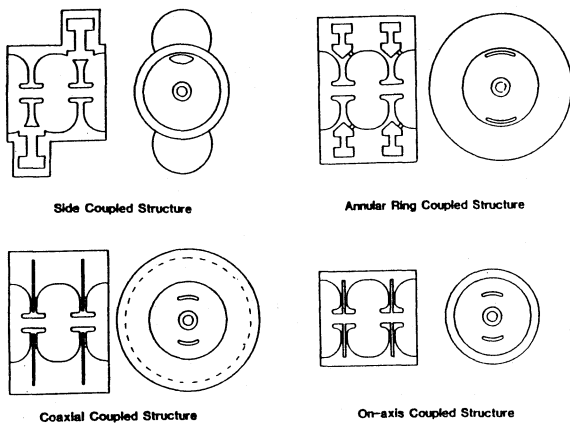


Figure 1. Various Standing-Wave Linear Accelerator Structures.

	Side Coupled	On-axis	Standard Coaxial	Annular Ring	New Design
Effective Diameter	16.5 cm	8.4 cm	12.6 cm	14.0 cm	8.4 cm
Minimum Web Thickness Between Accelerating Cells	3 mm	9 mm	9 mm	5 mm	9 mm
Maximum Nearest Neighbor Coupling: $K_1$	5 %	20 %	25 %	18 %	25 %
Nearest Neighbor Coupling = $K_1$ , Next Nearest Neighbor Coupling = $K_2$	30	200	-	-	110

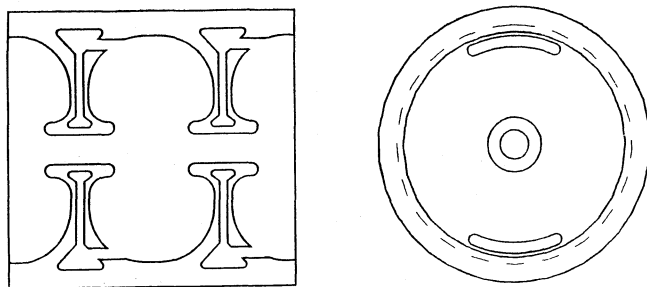


Figure 2. Schematic Illustration of New Coaxial Coupled Standing Wave Linear Accelerator Structure.

TABLE II DATA SUMMARY

Accelerator Length	35.9 cm
Number of Cavities	7½
Frequency	2997 MHz
Coupling: Nearest Neighbor ( $K_1$ )	3.3 %
Next Nearest Neighbor ( $K_2$ )	.03 %
RF Peak Power	2.3 MW
RF Pulsewidth	4.3 $\mu$ sec
$E_{peak}/E_0$	8.1
Transit Time Factor	.916
Theoretical $Q_0$	16,000
Theoretical $ZT^2/L$	124 Ma/m

	Design	Measured
$Q_0$	14,400	13,500
$Q_{ext}$	7,200	6,600
$\beta_0 = Q_0/Q_{ext}$	2.0	2.05
$ZT^2/L$	111 Ma/m	105 Ma/m

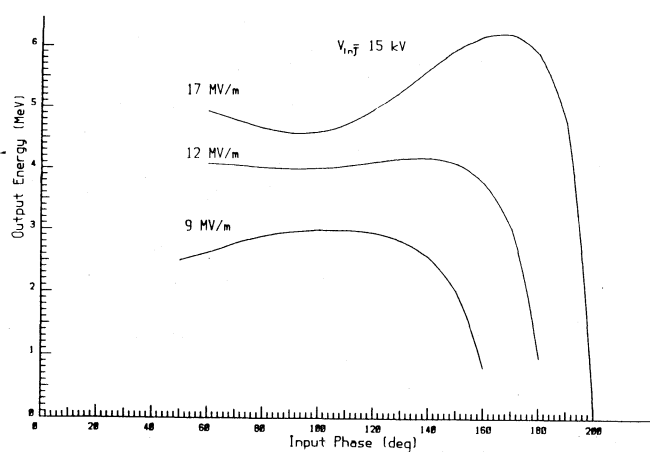


Figure 3. Energy Spectra of an S-Band Accelerator as a Function of Input Phase.

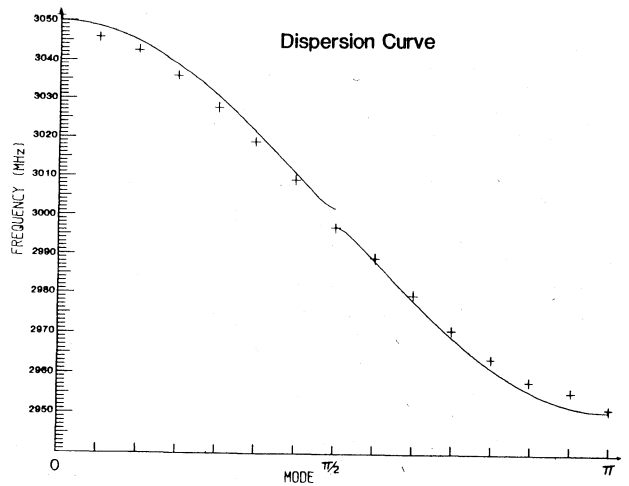


Figure 4. Dispersion Curve for an S-Band Coaxial Coupled Standing-Wave Accelerator.